

The Tokapal crater-facies kimberlite system, Chhattisgarh, India: reconnaissance petrography and geochemistry

Bernd Lehmann¹, Datta Mainkar², Boris Belyatsky³

¹Institute of Mineralogy and Mineral Resources, Technical University of Clausthal, Adolph-Roemer-Strasse 2a, 38678 Clausthal-Zellerfeld, Germany

²Directorate of Geology and Mining of Chhattisgarh, Raipur 492006 (Chhattisgarh), India

³Institute of Precambrian Geology and Geochronology, Russian Academy of Sciences, Makaraeva 2, 199034 St Petersburg, Russia

Abstract

The crater-facies kimberlite system at Tokapal occurs within the Late Proterozoic chemoclastic cover sequence of the Indravati Basin on the Meso-Proterozoic/Archaean Bastar craton in central India. The pyroclastic lapilli tuffs consist of pseudomorphs of olivine macrocrysts and juvenile lapilli set in a fine-grained talc-serpentine-carbonate matrix with locally abundant spinel and titanite. No garnets or diamonds have been found so far. The inequigranular and locally bedded texture is largely preserved, although the olivine component has been completely destroyed. The multiple kimberlite system has about circular shape (2.5 km in diameter) and is probably the oldest and largest crater-facies kimberlite system known in the world. The satellite Bhejripadar system of similar petrographic and chemical characteristics is situated about 4 km to the northwest and has a few hundred meters of diameter.

Samples from both systems have mostly moderate degree of contamination (35-50 wt% SiO₂, <4 wt% Al₂O₃) and Mg numbers of 82-89. The trace element patterns are typical of kimberlitic rocks (REE, Cr, Ni, Nb, Zr), with mobile elements strongly leached due to intense postmagmatic alteration and weathering (Ba, Sr, Rb, alkalis). The Nd isotope composition of ϵ_{Nd} around 2 (T=1100 Ma) is diagnostic of archetypal (Group I) kimberlites and similar to the diamondiferous Majhgawan pipe with ϵ_{Nd} 0 and the kimberlites of southern India with ϵ_{Nd} 2 (T=1080 Ma). The Early Paleozoic diamondiferous Kodomali kimberlite pipe from the nearby Mainpur kimberlite field also has ϵ_{Nd} 1 to 2 (T=480 Ma), suggestive of a slightly depleted to undifferentiated asthenospheric mantle source for all Indian kimberlitic rocks.

Introduction

The Tokapal system was hitherto mapped as an unspecified ultrabasic intrusion (Geological Survey of India 1979), but in the aftermath of the discovery of the diamondiferous Mainpur kimberlite field southeast of Raipur (Newlay and Pashine 1993) was reinterpreted as possible kimberlite by Sarkar (1995) and Verma (1995). A joint Indo-German remote sensing program allowed to better define the aerial extent of the Tokapal system, and also to locate the neighboring smaller Bhejripadar kimberlite pipe 4 km northwest (Bhattacharya et al. 1996). Exploration work of the Directorate of Geology and Mining during the last years has outlined the Tokapal system as probably the world's oldest and largest crater-facies kimberlite system (Mainkar et al. 2004).

Geologic situation

The Tokapal and Bhejripadar kimberlite systems occur within the Late Proterozoic chemoclastic platform sequence of the Indravati Basin on the Meso-Proterozoic/Archaean Bastar Craton, about 250 km south of Raipur and 20 km west of Jagdalpur (Fig. 1).

The basement geology consists largely of Meso-Proterozoic metagranites and gneisses, cut by NW trending dolerites (Mishra et al. 1988). The Bastar Craton is locally unconformably overlain by chemoclastic platform sedimentary rocks of the Indravati Supergroup. These undeformed cover rocks form the major Chhattisgarh Basin around Raipur, and the smaller Indravati and Khariar Basins 200 km south and 100 km southeast of Raipur, respectively. The stratigraphy of the Indravati Basin is detailed in Ramakrishnan (1987) and consists of the following sequence (from base to top):

Tirathgarh Formation (basal conglomerate and quartzite; 150-200 m), Cherakur Formation (micaceous purple shale; 50-60 m), Kanger Limestone (white to grey limestone; 50-60 m), Jagdalpur Formation (limestone, calcareous shale, sandstone intercalations; 150 m).

This sequence forms the lower Indravati Supergroup, a stratigraphic equivalent of the Vindhyan Supergroup. The minimum age of the basal portion of the Indravati Supergroup is constrained by the Rb-Sr isochron age (phlogopite) of 1067 ± 31 Ma from the Majhgawan kimberlite/lamproite pipe (Kumar et al. 1993) in central India which is emplaced in the Kaimur Sandstone, believed to represent a stratigraphic equivalent of the lowermost Indravati Supergroup (compare Sarkar et al. 1990). The only available absolute minimum age data from the basal Indravati Basin are from authigenic glauconitic minerals which yielded K-Ar ages of 700-750 Ma (Kreuzer et al. 1977).

The Tokapal system has a circular to elliptical shape with a diameter of about 2.5 km and presents a spectral anomaly in satellite imagery (Mainkar et al. 2004). The southeastern part of the intrusion is capped by several-m-thick laterite which stands out morphologically. The circular course of the small Bahar Nala (creek) marks the margin of the system. The river embankment also displays diagnostic outcrops in which grey-greenish stratified kimberlite tuff (dm- to m-thick "soapstone") is sandwiched in between the underlying grey to white Kanger Limestone and the overlying grey to purple shale of the Jagdalpur Formation (Fig. 1).

Exploration drilling has confirmed the presence of kimberlite lavas of more than 170 m thickness in the central part of the saucer-shaped system. The drillcores show that the kimberlite is composed of at least two different units separated by sandy material, and is confined to the stratigraphic interval in between the Cherakur and the Jagdalpur Formation (Mainkar et al. 2004).

Petrography

The rock is of a light to dark green colour and is characterized by angular and rounded black domains up to 15 mm large which locally are oriented and give the rock a slightly bedded aspect. These dark domains are olivine macrocrysts and pelletal lapilli which are entirely pseudomorphed by serpentine and talc, set in a dense grey-greenish groundmass (Fig. 2). The inter-clast and inter-lapilli matrix consists of serpentine/talc with euhedral sphene aggregates and opaques. Carbonate alteration is very pronounced in tuff layers which have abundant angular limestone clasts (Kanger Limestone). The fabric is very variable and ranges from densely to loosely packed and well to poorly sorted with macrocryst/lapilli aggregates mostly in the 0.4 to 2 mm range. Lapilli vary in shape from ovoid to more fluidal, irregular amoeboid forms. Olivine occurs in

two populations, i.e. subhedral to rounded macrocrysts up to 15 mm large, and a fine-grained euhedral population with <0.5 mm in size. The inter-clast and inter-lapilli matrix is composed of dense, often massive serpentine-talc aggregates.

The neighboring Bhejripadar system forms a circular morphological depression of about 600 m in diameter within purple shale of the Cherakur Formation. This system is even more weathered than Tokapal, and the surface rocks are greyish to yellowish in colour (yellow ground). However, there is still a relic bedded pyroclastic texture preserved.

Neither system has olivine preserved in the thin sections studied. No garnet or diamond have been found so far. Microdiamond testing of two 18 kg bulk samples by Lakefield Research Ltd (Lakefield, Ontario, Canada) proved negative. The textural identification as kimberlite is according to features which are very close to the FALC kimberlite field, Saskatchewan, Canada, and other crater-facies kimberlite systems as described and documented in Mitchell (1995, 1997). The petrological identification as kimberlite is from chemical and Nd isotope data.

Geochemistry

Chemical bulk-rock data from Tokapal and Bhejripadar plus some reference data from the diamondiferous Kodomali (Mainpur kimberlite field) and Majhgawan systems (central India) are given in Table 1. Although all rock samples from Tokapal and Bhejripadar are heavily altered and have consequently undergone significant changes in their major and trace element composition, particularly loss of mobile alkali and alkaline earth elements (Na, K, Rb, Ca, Sr, Ba), the more immobile elements such as Ti, Cr, Ni, Nb, Zr, REEs allow petrogenetic conclusions.

The samples analyzed from Tokapal and Bhejripadar are relatively homogeneous, in spite of large textural variability. The Tokapal samples have a low to moderate degree of contamination (C.I. mostly 1.0 to 1.3) as seen in the $\text{SiO}_2\text{-Al}_2\text{O}_3$ plot of Fig. 3. The three samples which plot near 50 wt% SiO_2 are from a soapstone-like tuff layer exposed at the embankment of the Bahar Nala creek. The Bhejripadar samples plot similar to the Tokapal soapstone/tuff layer and display a similar degree of contamination with C.I. around 2.0. Both systems are low in aluminum, typical of kimberlites but different from lamproites (Fig. 3).

A remarkable feature of the Majhgawan reference samples (Table 1) is their elevated titanium at low potassium content (>5 wt% TiO_2 at <2 wt% K_2O) which is a typical feature of some kimberlites but does not occur in orangeites and lamproites (Smith et al. 1985). All samples analyzed have high magnesium content (>25 wt% MgO , i.e. >30 wt% MgO if recalculated on an anhydrous basis) which combined with a low alumina content (<4 wt% Al_2O_3 for Tokapal and Bhejripadar) characterizes a kimberlitic or unevolved lamproitic composition (Fig. 4).

The Zr-Nb plot defines a kimberlitic affinity for the Tokapal, Bhejripadar and Kodomali samples while the very high Zr content of the Majhgawan samples is a distinctive feature of lamproites (Fig. 5). The REE patterns are typical of alkaline rocks in general and reflect the strong enrichment in LREEs of such rocks. The samples from Tokapal, Bhejripadar and Kodomali have congruent distribution patterns. The Majhgawan samples have a particularly fractionated REE pattern with a degree of LREE enrichment typical of lamproites.

Neodymium and some strontium isotope data are listed in Table 2. The initial isotope ratios for Tokapal, Bhejripadar and Majhgawan are calculated for an age

of 1100 Ma which seems to broadly apply to Majhgawan and the southern Indian kimberlites (Kumar et al. 1993), and which is also thought to be close to the stratigraphic age of the Tokapal and Bhejripadar systems. Three samples from the Tokapal and Bhejripadar systems have ϵ_{Nd} values in between 1.7 to 2.9. However, one sample gives an anomalously high ϵ_{Nd} value of 9.6 for $T=1100$ Ma which indicates either a disturbance of the Sm-Nd isotope system, or a younger overprint/magmatic event. The two Kodomali samples from the recently discovered diamondiferous Mainpur kimberlite field, about 130 km north of the Tokapal field, also have a very high $^{143}Nd/^{144}Nd$ ratio which excludes an old age in the 1100 Ma range (ϵ_{Nd} 10 to 12 for $T=1100$ Ma). This system thus must be considerably younger. A more realistic initial ϵ_{Nd} around 4 requires an age of 600 Ma, whereas an ϵ_{Nd} around 2 as for the other central and southern Indian kimberlite systems (Basu and Tatsumoto 1979; Chalapathi Rao et al. 1998) would give an age of 500 Ma. Recent whole-rock Ar-Ar dating of a Kodomali sample by Chalapathi Rao et al. (2005) has indeed demonstrated a plateau age of 478 ± 2 Ma which is interpreted as maximum age of kimberlite emplacement. It could well be that the same kimberlitic event seen at Kodomali also is expressed by the one anomalous sample at Tokapal.

The chondritic to positive time-corrected ϵ_{Nd} values of the samples analyzed indicate a slightly depleted athenospheric mantle source. This is the main criterion for archetypal kimberlites (Group I kimberlite) (Mitchell 1995; Mitchell and Bergman 1991), and is distinctly different from Group II kimberlites (orangeite clan) or lamproites which have a source located in the non-convecting continental lithospheric mantle, invariably reflected by negative ϵ_{Nd} values of less than -5 (Smith 1983). These negative ϵ_{Nd} values of -6 to -14 in orangeites and lamproites correlate with a radiogenic Sr isotope composition of ≥ 0.707 (Mitchell 1995) which is not seen in our limited data set.

Conclusions

The Tokapal-Bhejripadar systems vary in between the end-members of juvenile lapilli-dominated and olivine-dominated kimberlite tuffs. The pyroclastic components are dominated by varying proportions of fine- to medium-grained lapilli and olivine macrocrysts. The textural and chemical features all point to the Tokapal and Bhejripadar systems being volcanoclastic Group 1 kimberlites of crater facies.

Similar systems are known from the 100 Ma-old diamondiferous Fort à la Corne (FALC) kimberlite field, Saskatchewan, Canada (Field and Scott Smith 1999; Berryman et al. 2004). The FALC kimberlites are xenolith-poor, have a wide range of textural composition and a narrow range in chemical composition. They have shallow champagne glass-shape with diameters ranging up to 1300 m and depths mostly less than 200 m below a 100 m-thick glacial overburden. No diatreme or root zones or related textural types of kimberlites have been found so far (Berryman et al. 2004). The Upper Cretaceous-Tertiary highly diamondiferous Lac de Gras kimberlites in the NWT, Canada, partly also consist of volcanoclastic infill but are much steeper and smaller pipes with a high amount of xenocrysts.

No diamond or garnet is known from the Tokapal and Bhejripadar systems. The occurrence of garnet is commonly regarded a prerequisite for the formation of diamond deposits because diamonds are derived from disaggregated xenoliths of peridotitic and eclogitic material sampled by a kimberlite magma during its ascent (Gurney and Switzer 1973). However, the abundance of garnet is very variable in between different kimberlite systems and is neither related to kimberlite chemistry nor diamond content. Garnet can be very rare in some

diamondiferous kimberlite systems, such as those from the Arkhangelsk province, Russia, with <1 to 5 ppm garnet only (Krotkov et al. 2001).

The stratigraphic age of the Tokapal and Bhejripadar kimberlite systems corresponds to the age of the diamondiferous Majhgawan pipe of central India and to the diamondiferous kimberlites of southern India. The very broad extent and favorable geological setting warrant a prolonged exploration effort, particularly in the light of the multiple nature of the system which may reflect superimposed kimberlitic events of possibly widely different age.

Acknowledgements

This study was initiated by the joint Indo-German project on "Improved mineral exploration model development" between Deutsche Gesellschaft für Technische Zusammenarbeit (GTZ) and the National Remote Sensing Agency of India (NRSA). Field work was supported by the Directorate of Geology and Mining, Madhya Pradesh. We thank Prof Franz List, Free University of Berlin, for guidance in an early stage of the cooperation project. Three reference samples from Majhgawan were provided by Dr Dhanapati Haldar, Hyderabad.

References

- Basu A.R., Tatsumoto M. (1979) Samarium-neodymium systematics in kimberlites and in the minerals of garnet lherzolite inclusions. *Science* 205: 398-401
- Berryman A.K., Scott Smith B.H., Jellicoe B.C. (2004) Geology and diamond distribution of the 140/141 kimberlite, Fort à la Corne, central Saskatchewan, Canada. *Lithos* 76: 99-114

Bhattacharya A., Kamaraju M.V.V., Dangwal M., Shrivastav N.S., Mainkar D., Tiwari R., Singh H.P. (1996) IRS-1C discovers a new kimberlite pipe for diamond exploration. *Interface* <Bull NRSA Data Centre, Hyderabad> 7 (4): 7-8

Chalapathi Rao N.V., Gibson S.A., Pyle D.M., Dickin A.P. (1998) Contrasting isotope mantle sources for Proterozoic lamproites and kimberlites from the Cuddapah Basin and Eastern Dharwar Craton: implication for Proterozoic mantle heterogeneity beneath southern India. *J. Geol. Soc. India* 52: 683-694.

Chalapathi Rao N.V., Burgess R., Anand M., Mainkar D. (2005) Evidence for a Phanerozoic (478 Ma) diamondiferous kimberlite emplacement epoch in the Indian shield from $^{40}\text{Ar}/^{39}\text{Ar}$ dating of the Kodomali kimberlite: implications for Pan-African thermo-tectonic imprints in the Bastar craton and Rodinia tectonics. *Geol. Soc. India*, mscr. submitted

Field M., Scott Smith B. (1999) Contrasting geology and near-surface emplacement of kimberlite pipes in Southern Africa and Canada. In: Gruney J.J., Gurney J.L., Pascoe M.D., Richardson S.H. (eds.), *Proceedings VII Intern. Kimberlite Conf.* 1: 214-236.

Geological Survey of India (1979) Geological Quadrangle Map 1:253,440. Kondagaon quadrangle 65E.

Gurney J.J., Switzer G.S. (1973) The discovery of garnets closely related to diamonds in the Finsch pipe, South Africa. *Contr. Mineral. Petrol.* 39: 103-116.

Kreuzer, H., Harre, W., Kürsten, M., Schnitzer, W.A., Murti, K.S., Srivastava, N.K. (1977) K-Ar dates of two glauconites from the Chandarpur Series (Chhattisgarh/India). *Geol. Jb.* B28: 23-36

Krotkov V.V., Kudriavtseva O.A., Bogatikov O.A., Valuev E.P., Verzhak V.V., Garanin V.K., Zaostrovsev A.A., Kononova V.A., Litinsky Y.V.,

- Pashkevich I.R., Stepanov A.N., Fortygin V.S. (2001) New technologies of diamond exploration. Moscow, Geos, 310 p.
- Kumar A., Padma Kudmari V.M., Dayal A.M., Murthy D.S.N., Gopalan K. (1993) Rb-Sr ages of Proterozoic kimberlites of India: evidence for contemporaneous emplacement. *Precambrian Research* 62: 227-237.
- Mainkar D., Lehmann B., Haggerty S.E. (2004) Discovery of the very large crater-facies kimberlite system of Tokapal, Bastar district, Chhattisgarh, India. *Lithos* 76: 201-217.
- Mishra V.P., Singh P., Dutta N.K. (1988) Stratigraphy, structure and metamorphic history of Bastar craton. *Geol. Surv. India, Rec.* 117 (3-8): 1-26
- Mitchell R.H. (1986) Kimberlites. Mineralogy, geochemistry, and petrology. New York-London, Plenum Press, 442 p.
- Mitchell R.H. (1995) Kimberlites, orangeites, and related rocks. Plenum Press, New York-London, 410 p.
- Mitchell R.H. (1997) Kimberlites, orangeites, lamproites, melilitites, and minettes: a petrographic atlas. Almaz Press, Thunder Bay, 243 p.
- Mitchell R.H., Bergman S.C. (1991) Petrology of lamproites. Plenum Press, New York, 447 p.
- Newlay S.K., Pashine J. (1993) New find of diamond-bearing kimberlite in Raipur district, Madhya Pradesh, India. *Curren Science* 65 (4): 292-293.
- Ramakrishnan M. (1987) Stratigraphy, sedimentary environment and evolution of the Late Proterozoic, Indravati Basin, Central India. *Geol. Surv. India, Spec. Publ.* 28: 139-160.
- Sarkar S.K. (1995) Kimberlite discoveries in Raipur district and initiation of exploration for diamond in so far unexplored areas of Raipur-Raigarh-Bastar districts, Madhya Pradesh. *Seminar on Diamond Exploration, Hyderabad*, 11 p.

- Sarkar A., Sarkar G., Paul D.K., Mitra N.D. (1990) Precambrian geochronology of the central Indian shield. A review. Geol. Surv. India, Spec. Publ. 28: 453-482.
- Scott Smith B.H. (1996) Kimberlites. In: Mitchell, R.H., ed., Undersaturated alkaline rocks: mineralogy, petrogenesis, and economic potential. Mineral. Assoc. Canada, Short Course Volume 24: 217-243.
- Smith C.B. (1983) Pb, Sr, and Nd isotopic evidence for sources of African Cretaceous kimberlites. Nature 304: 51-54.
- Smith C.B., Gurney, J.J., Skinner, E.M.W., Clement, C.R., Ebrahim, N. (1985) Geochemical character of South African kimberlites: a new approach based on isotopic constraints. Transact. Geol. Soc. S. Afr. 88: 267-280.
- Taylor S.R., McLennan S.M. (1985) The continental crust: its composition and evolution. Blackwell, Oxford, 312 p.
- Verma S. (1995) Geological observation note on ultrabasic intrusive of Tokapal, Bastar district, M.P. Unpubl. report, DGM, Raipur.

Legends to Figures and Tables

Fig. 1. Geologic setting of the Tokapal and its satellite Bhejripadar kimberlite system in the Late Proterozoic Indravati Basin on the Bastar Craton.

Fig. 2. Rock fabrics in thin sections of typical samples from the Tokapal kimberlite system compared to the Kodomali kimberlite pipe and the diamondiferous Fort à la Corne (FALC) crater-facies kimberlite in Saskatchewan, Canada.

A: Loosely packed, resedimented (?) pelletal lapilli and pseudomorphed olivine macrocrysts in serpentine-talc matrix (Tokapal, sample D, plane light); B: Loosely packed faintly bedded volcanoclastic kimberlite with carbonatized pelletal lapilli/olivine macrocrysts (Tokapal, sample G, plane light); C: Lobate-shaped fluidal lapillum with core consisting of serpentinized olivine and kimberlitic selvage zone (dark) rich in opaques (Tokapal, sample C, plane light); D: Euhedral titanite in strongly altered kimberlite tuff with leached open spaces (white) (Bhejripadar, sample BP1a, plane light); E: Hypabyssal kimberlite with olivine macro- and microcrysts in fine-grained dark matrix (Kodomali, sample K1, crossed nicols); F: Crater-facies kimberlite with juvenile lapilli and olivine macrocrysts (FALC, sample 168-1G, plane light).

Fig. 3. SiO_2 versus Al_2O_3 plot for some Indian kimberlite systems. Reference data for contamination-free kimberlites from Mitchell (1986: 278), average kimberlite from Scott Smith (1996: 219), average lamproite from Mitchell and Bergman (1991: 311).

Fig. 4. $\text{MgO}-\text{Al}_2\text{O}_3-\text{K}_2\text{O}$ triangle plot (reference data from Mitchell 1986; Mitchell and Bergman 1991; Scott Smith 1996).

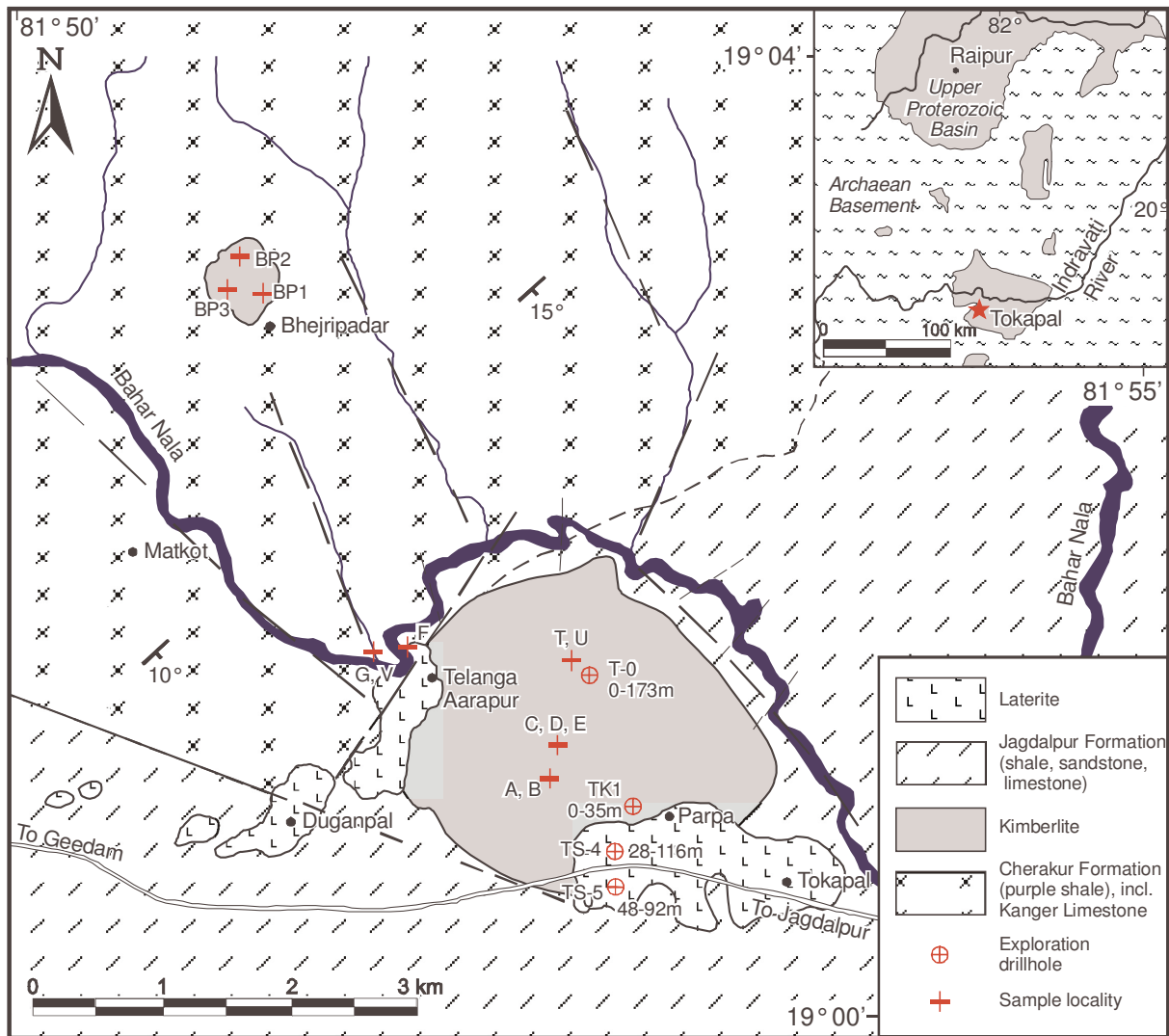
Fig. 5. Nb versus Zr plot (reference data from Mitchell 1986; Mitchell and Bergman 1991; Scott Smith 1996).

Fig. 6. REE plot of some Indian kimberlites (reference data from Taylor and McLennan 1985).

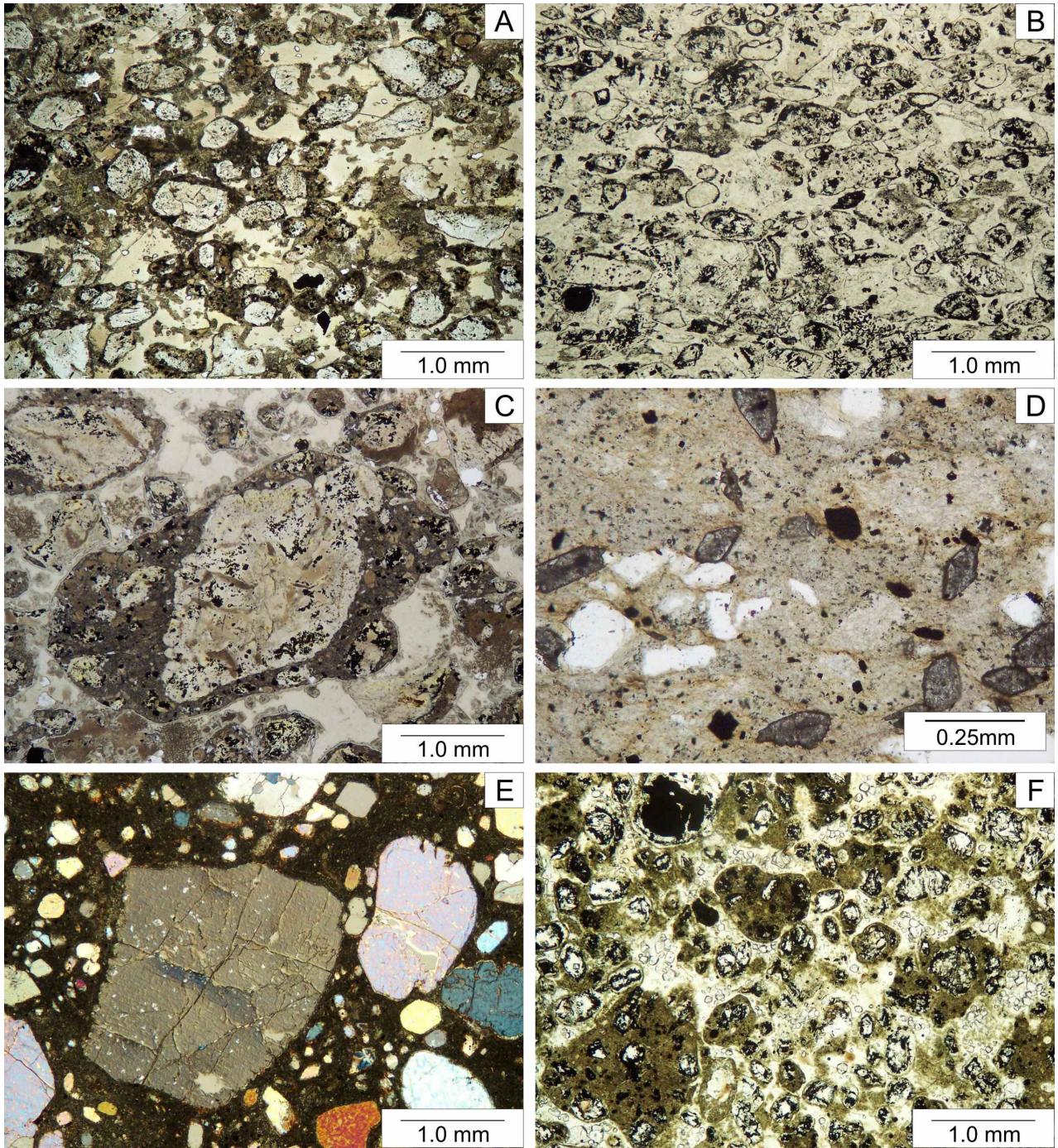
Fig. 7. Initial Sr versus Nd isotope ratios of some Indian kimberlites compared to MORB and other alkaline ultramafic rock types and provinces (adapted from Mitchell and Bergman 1991: 347). FALC data from Lehmann (unpublished).

Table 1. Bulk-rock chemical data (C.I.=Contamination Index = $(\text{SiO}_2 + \text{Al}_2\text{O}_3 + \text{Na}_2\text{O}) / (\text{MgO} + \text{K}_2\text{O})$, wt%; Mg# = $\text{Mg} / (\text{Mg} + \text{Fe}) \times 100$, at%)

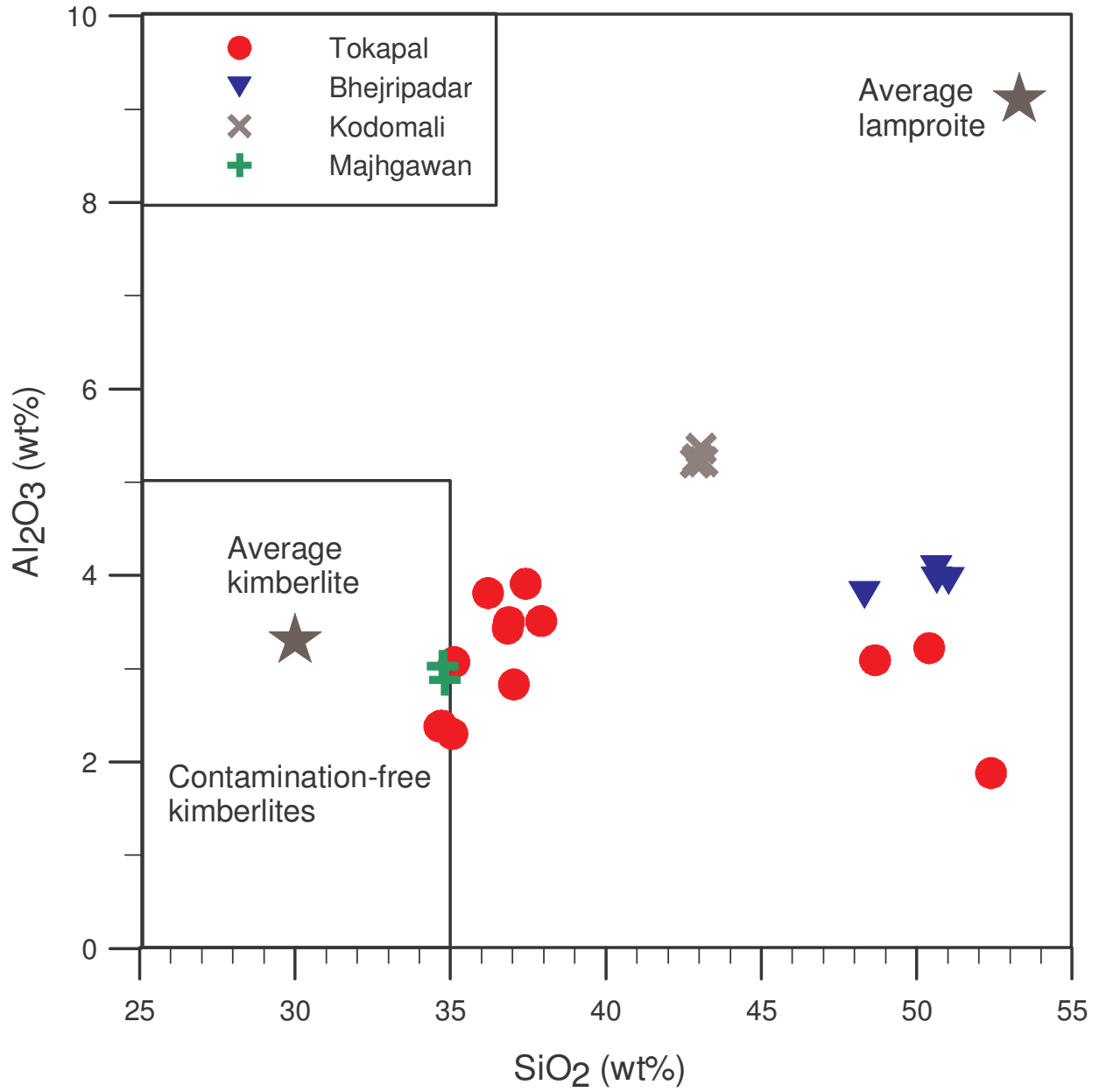
Table 2. Nd and Sr isotope data on some Indian kimberlites



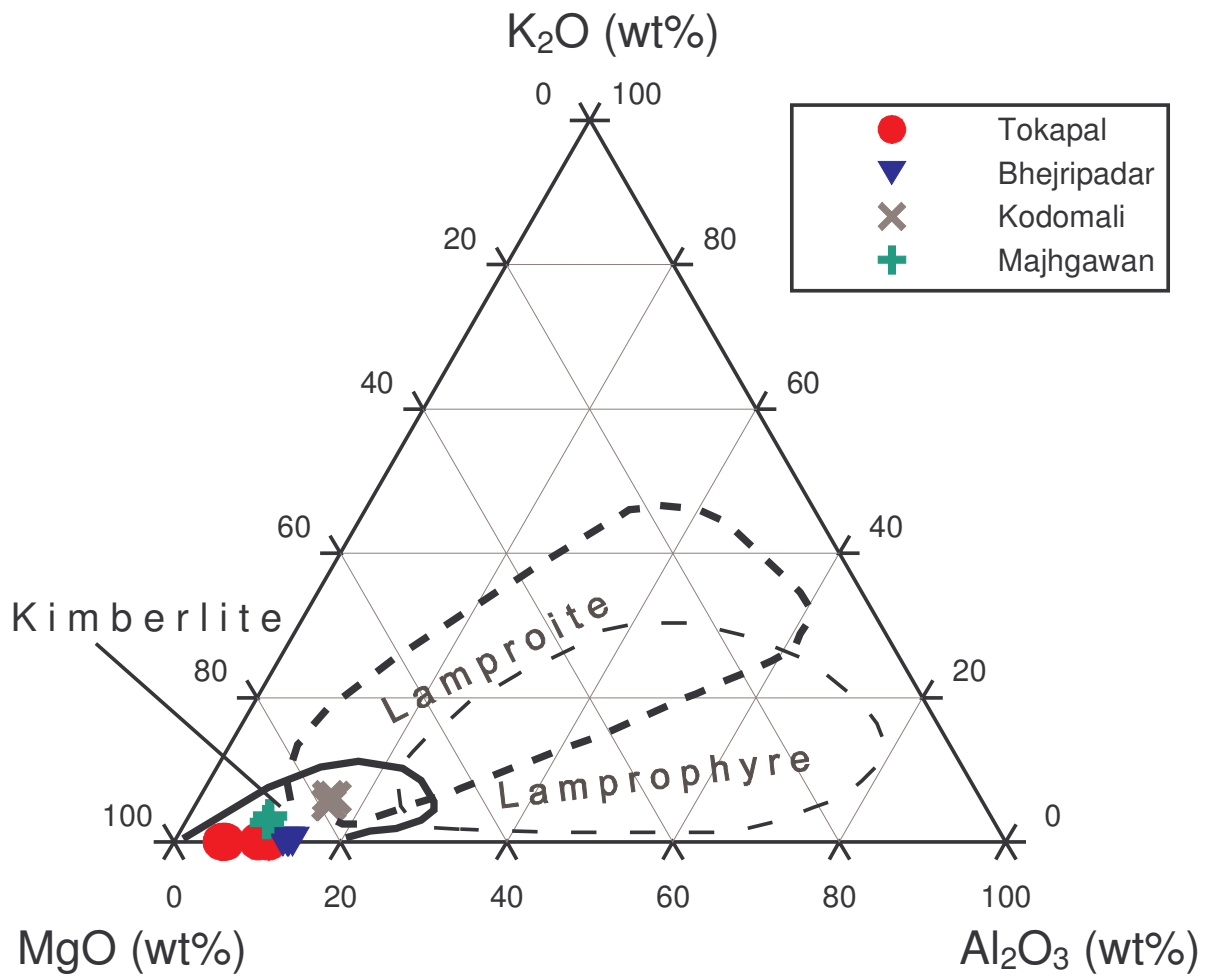
Lehmann et al.: Figure 1



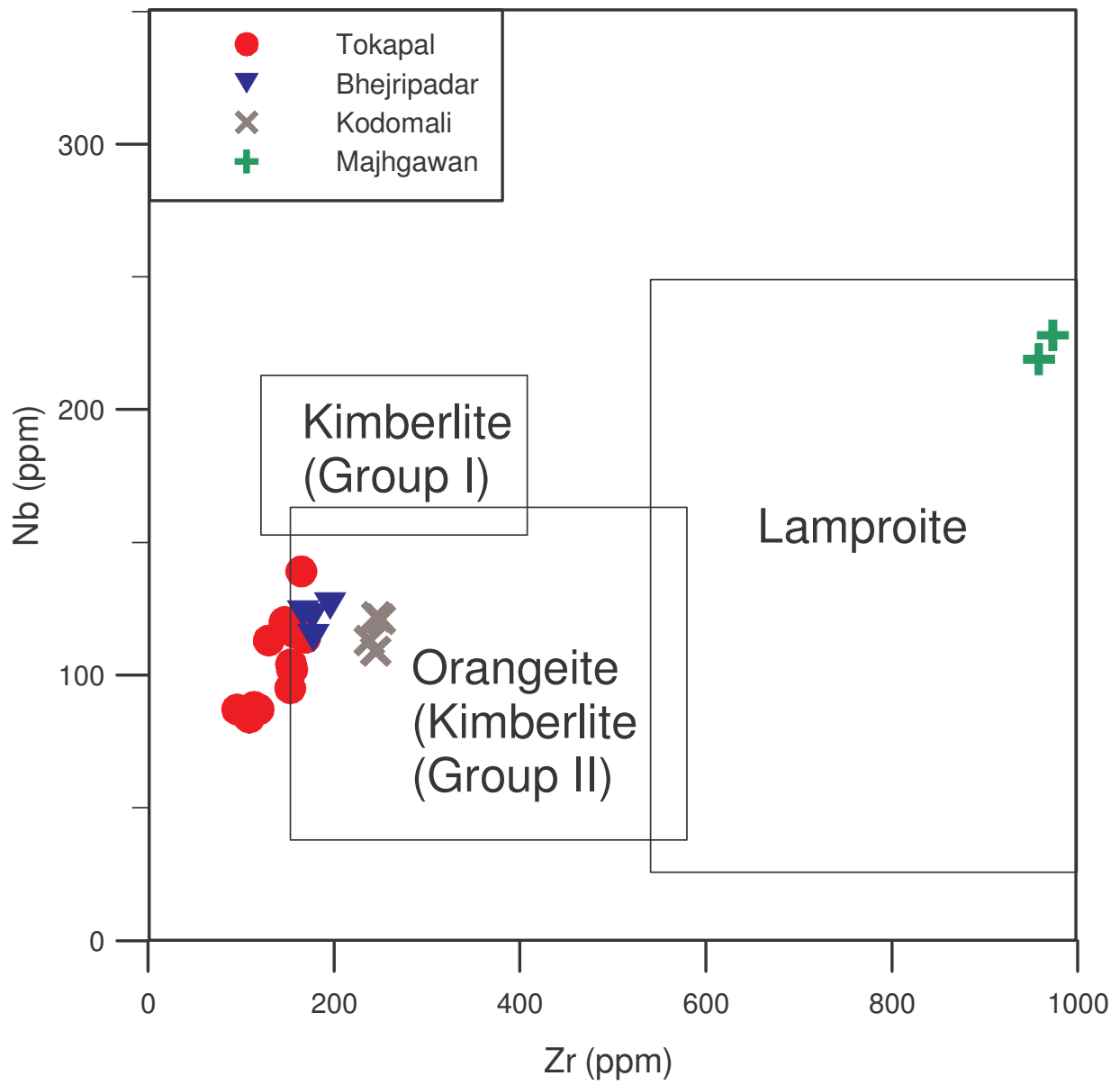
Lehmann et al.: Figure 2



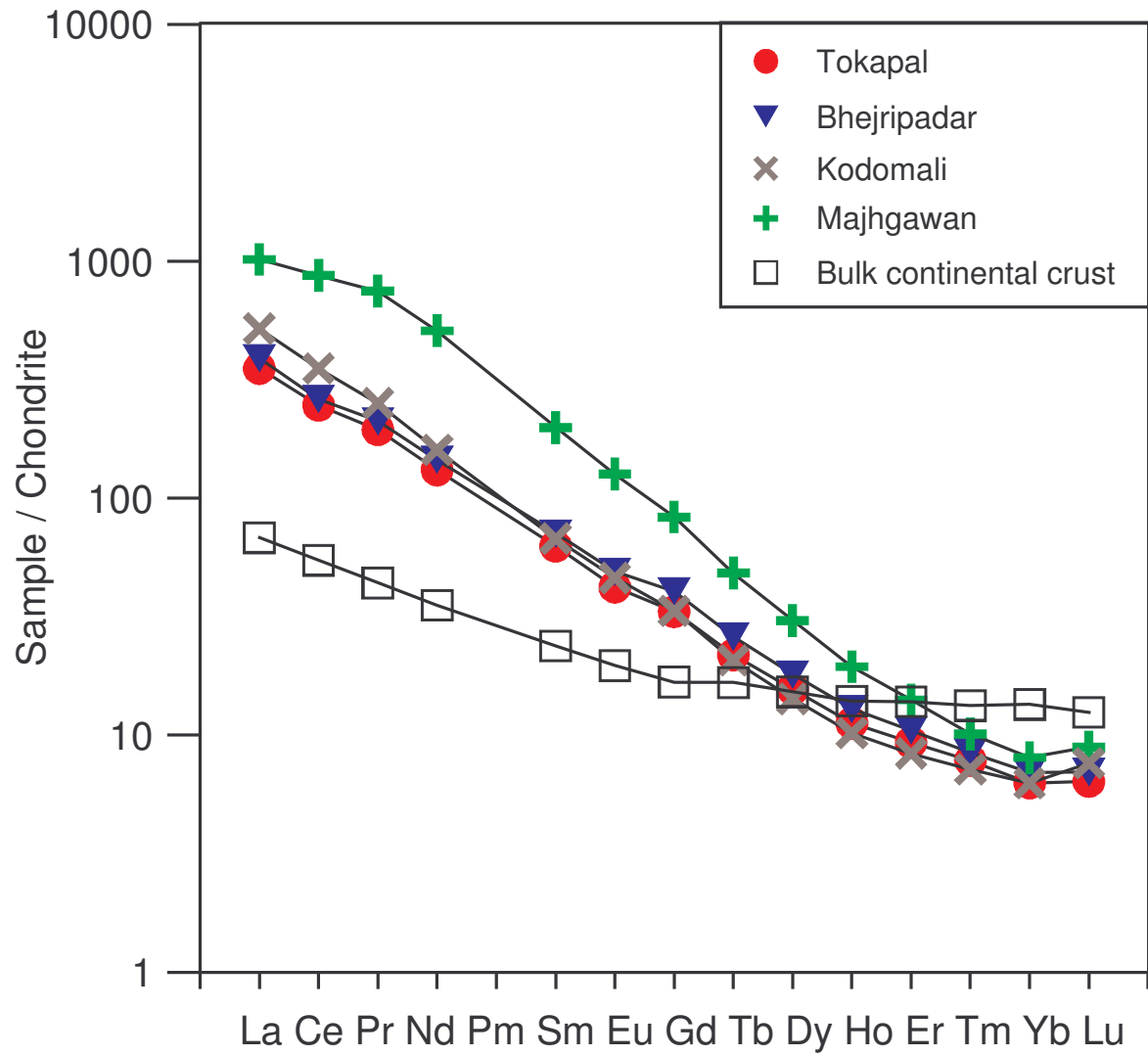
Lehmann et al.: Fig. 3



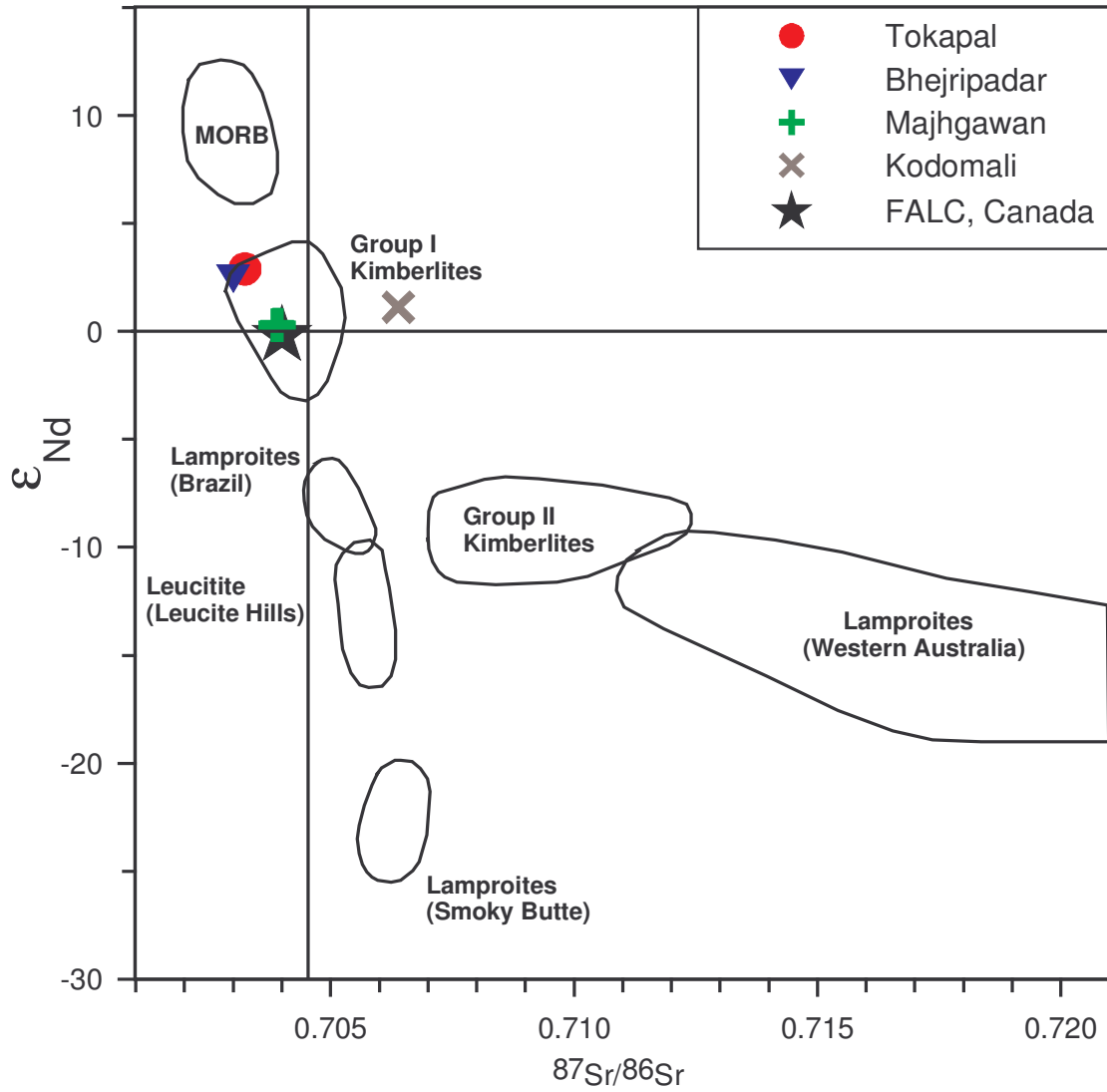
Lehmann et al: Fig. 4.



Lehmann et al: Fig. 5



Lehmann et al: Fig. 6



Lehmann et al: Fig. 7

Lehmann et al: Table 1

Sample	SiO ₂ wt% XRF	TiO ₂ wt% XRF	Al ₂ O ₃ wt% XRF	Fe ₂ O ₃ wt% XRF	MnO wt% XRF	MgO wt% XRF	CaO wt% XRF	Na ₂ O wt% XRF	K ₂ O wt% XRF	P ₂ O ₅ wt% XRF	LOI wt% GRAV	Total wt%	C.I.	Mg#
Tokapal														
A1	36.21	2.22	3.81	12.69	0.21	30.93	0.77	<0.01	0.01	0.51	12.32	99.81	1.29	83
B1	37.42	1.89	3.91	10.15	0.19	32.35	0.64	<0.01	0.01	0.42	12.63	99.73	1.28	86
C1	36.88	2.03	3.50	12.59	0.21	30.71	0.74	<0.01	0.01	0.51	12.58	99.90	1.31	83
D1	36.84	2.15	3.43	11.17	0.17	31.61	1.12	<0.01	0.01	0.58	12.53	99.74	1.27	85
E1	37.92	1.98	3.51	10.39	0.22	31.69	0.72	0.01	0.01	0.51	12.70	99.78	1.31	86
F1	48.66	2.48	3.09	11.34	0.02	26.85	0.64	<0.01	0.01	0.51	5.93	99.62	1.93	82
G1	37.04	2.10	2.83	10.87	0.12	25.15	6.32	0.03	0.01	0.52	13.52	98.97	1.59	82
T	35.12	2.41	3.07	11.17	0.16	27.35	8.27	0.01	0.02	0.59	11.24	99.47	1.39	83
U1	34.64	1.79	2.38	10.87	0.20	36.73	0.97	0.02	0.01	0.44	12.32	100.31	1.01	87
U2	34.71	1.74	2.39	10.45	0.20	37.28	0.67	0.01	0.01	0.41	12.21	100.07	1.00	88
U3	35.06	1.89	2.30	9.53	0.20	37.94	0.71	0.01	0.01	0.40	12.22	100.25	0.99	89
V1	52.39	1.67	1.88	10.37	0.02	28.33	<0.01	0.04	0.01	0.04	5.45	100.19	1.92	84
V2	50.40	2.71	3.22	12.09	0.14	25.05	0.04	0.04	0.01	0.05	6.19	99.90	2.14	80
Bhejripadar														
BP1	50.63	2.48	4.07	9.60	0.03	24.45	0.83	0.17	0.02	0.56	6.69	99.57	2.24	83
BP1a	50.64	2.46	3.95	8.79	0.05	25.04	1.49	0.11	0.01	0.55	6.35	99.45	2.18	85
BP2a	51.02	2.22	3.94	8.90	0.07	24.69	1.37	0.02	0.01	0.57	6.69	99.50	2.23	85
BP3	48.32	2.41	3.79	9.91	0.10	25.12	0.99	0.02	0.02	0.61	8.12	99.43	2.07	83
Kodomali														
K3	42.96	1.25	5.25	8.84	0.14	25.61	8.16	1.11	1.71	0.43	3.43	98.91	1.70	85
K4	43.06	1.24	5.36	8.74	0.14	25.49	7.95	1.08	2.01	0.38	3.41	98.88	1.68	85
K7	43.12	1.26	5.22	8.28	0.14	25.87	8.54	1.06	1.72	0.45	3.70	99.34	1.79	86
K8	42.89	1.29	5.21	7.94	0.14	26.34	8.61	0.99	2.11	0.40	3.29	99.20	1.73	87
Majhgawan														
M	34.82	5.70	2.88	10.49	0.19	25.73	3.63	0.26	0.81	2.47	11.84	98.94	1.39	83
M1	34.75	5.69	3.03	8.79	0.13	26.88	3.32	0.05	1.11	2.42	12.28	98.90	1.35	86

Sample	Ba ppm ICPMS	Co ppm XRF	Cr ppm XRF	Cu ppm XRF	Ga ppm XRF	Hf ppm ICPMS	Nb ppm XRF	Ni ppm XRF	Pb ppm ICPMS	Rb ppm ICPMS	Sc ppm XRF	Sr ppm ICPMS	Ta ppm XRF	Th ppm ICPMS	U ppm ICPMS	V ppm XRF	Y ppm ICPMS	Zn ppm XRF	Zr ppm XRF
Tokapal																			
A1	41	65	1126	74	6	6.20	115	1197	47.1	<1	16	27.1	<5	17.4	1.7	42	17	84	168
B1	41	74	1002	52	8	5.00	95	1364	51.1	<1	14	20.7	<5	16.2	1.6	83	15.5	70	153
C1	53	73	1017	61	5	5.10	102	1180	15.2	<1	11	23.1	7	17	2.1	27	15.5	85	155
D1	43	56	1076	57	6	4.80	114	1220	11.9	<1	16	29.3	<5	15.9	2.1	43	17.1	73	169
E1	51	72	992	64	5	5.30	104	1274	9.07	<1	15	22	9	16.3	2.17	24	16.2	67	154
F1	54	87	1739	10	7	4.68	116	1239	17.4	<1	15	16.1	<5	15.2	2.18	67	23.1	232	158
G1	5511	64	1197	<10	3	4.18	113	921	26.5	<1	14	12.8	<5	14	1.79	86	14	117	130
T	97	74	1340	88	7	4.11	120	1216	<4	1.41	18	80.7	<5	12.7	1.48	55	16.5	92	147
U1	24	94	993	37	8	3.40	87	1121	17	<2	13.1	21	6	11.7	1.8	44	13	40	119
U2	24	102	952	25	8	3.10	84	1222	50	<2	12.6	20	5	11.5	1.3	42	12	45	109
U3	21	91	1030	66	7	3.30	88	1487	7	<2	13.3	22	7	11.5	1.7	41	13	39	114
V1	40	71	1350	32	7	3.10	87	961	14	<2	10.8	4	5	10.5	1.5	55	14	205	96
V2	99	140	1250	6	12	4.70	139	1599	20	<2	17.7	4	10	17	3.9	143	18	232	165
Bhejripadar																			
BP1	31	41	1405	56	4	5.43	126	880	9.55	0.43	17	17.4	7	16.3	2.4	208	24.2	98	196
BP1a	77	73	1379	82	6	5.38	122	932	4.57	0.65	18	19	<5	16.5	2.15	209	16.5	87	177
BP2a	50	60	1217	67	5	5.43	114	857	48.6	0.23	14	19.5	10	17.2	2.14	111	19.4	77	178
BP3	20	54	1369	87	7	5.29	123	1653	22.8	1.98	18	27.6	6	16	2.63	145	19.2	72	167
Kodomali																			
K3	2773	83	1744	71	8	6.68	109	1209	8.25	87.9	17	982	<5	18.4	3.03	118	14.8	65	245
K4	2803	77	1763	69	6	6.48	113	1178	22.4	90.4	15	948	<5	18.2	3	121	14.5	69	238
K7	3898	77	1690	46	7	6.30	121	884	5	81.0	15.7	1078	5	17.9	3.2	107	14	46	250
K8	3299	76	1690	44	8	6.50	122	906	<5	90.0	15.8	1052	6	18.3	3.3	108	16	48	246
Majhgawan																			
M	1734	82	996	52	7	5.10	228	1071	23.5	56.3	19	1694	16	16.2	3.49	33	26.5	85	973
M1	1867	110	948	31	10	18	219	1189	23	65	20	1516	11	23	8	60	18	81	958

Lehmann et al: Table 1 (continued)

Sample	La	Ce	Pr	Nd	Sm	Eu	Gd	Tb	Dy	Ho	Er	Tm	Yb	Lu
	ppm ICPMS	ppm ICPMS	ppm ICPMS	ppm ICPMS	ppm ICPMS	ppm ICPMS	ppm ICPMS	ppm ICPMS	ppm ICPMS	ppm ICPMS	ppm ICPMS	ppm ICPMS	ppm ICPMS	ppm ICPMS
Tokapal														
A1	93.8	172	20.1	68.8	10.2	2.63	6.94	0.841	3.98	0.674	1.52	0.182	1.01	0.151
B1	79	145	17	57	9	2.33	6.02	0.702	3.55	0.594	1.42	0.185	0.976	0.144
C1	89.5	159	18.2	60.7	9.13	2.19	6.29	0.745	3.58	0.554	1.37	0.173	0.966	0.132
D1	96.2	164	19	63.5	9.59	2.53	6.59	0.802	3.84	0.641	1.44	0.188	0.941	0.145
E1	76.9	139	16.1	54.4	8.3	2.06	6.11	0.753	3.57	0.613	1.46	0.181	0.95	0.145
F1	83.4	161	19.3	69.1	11.2	2.98	8.4	0.991	4.83	0.813	1.95	0.254	1.41	0.218
G1	62.7	104	12.2	43.6	7.18	1.64	5.33	0.641	3.22	0.52	1.27	0.169	1.01	
T	80.4	143	16.6	58	9.12	2.49	6.68	0.799	3.82	0.618	1.42	0.167	0.93	0.137
U1	71.3	121		50	6.8	2.1		<0.5					0.7	0.11
U2	68.3	115		46	6.8	2.0		<0.5					0.7	0.11
U3	73.2	116		53	7.4	2.1		<0.5					0.7	0.10
V1	73.1	116		54	7.4	1.9		<0.5					0.9	0.14
V2	104	188		82	9.6	2.8		<0.5					1.1	0.15
Bhejripadar														
BP1	101	169	20.7	73.8	12.2	3.28	10.2	1.150	5.40	0.884	1.99	0.234	1.29	0.195
BP1a	93.8	141	17.1	59.5	9.55	2.57	6.78	0.815	3.78	0.618	1.46	0.180	1.10	0.156
BP2a	93.8	167	18.6	64.1	9.74	2.48	7.28	0.872	4.05	0.674	1.55	0.196	1.05	0.159
BP3	91.8	156	18.8	65.2	10.2	2.64	7.65	0.910	4.32	0.714	1.66	0.201	1.09	0.161
Kodomali														
K3	122	213	22.4	72.3	9.93	2.58	6.59	0.745	3.46	0.572	1.33	0.172	1.02	0.183
K4	120	210	22.3	71.9	9.83	2.54	6.58	0.747	3.49	0.556	1.33	0.167	1.01	0.181
K7	134	216		80	10.4	2.8		<0.5					1.0	0.16
K8	135	212		77	10	2.8		<0.5					0.9	0.14
Majhgawan														
M	239	525	66.6	230	29.2	7.08	16.4	1.74	7.41	1.09	2.24	0.243	1.31	0.214
M1	229	428		186	24.5	4.0		1.4					1.5	0.25

Lehmann et al: Table 2

Sample	Age	[Sm]	[Nd]	$^{147}\text{Sm}/^{144}\text{Nd}$	$^{143}\text{Nd}/^{144}\text{Nd}$	2s	ϵ	T(DM)	T(DM2)	[Rb]	[Sr]	$^{87}\text{Rb}/^{86}\text{Sr}$	$^{87}\text{Sr}/^{86}\text{Sr}$	2s	$(^{87}\text{Sr}/^{86}\text{Sr})_t$
Tokapal															
V1	1100	7.391	54.34	0.08223	0.511959	11	2.9	1381	1494	1.843	4.691	1.137	0.707367	25	0.689472
U1	1100	6.837	50.12	0.08247	0.512306	15	9.6	982	935	4.012	23.69	0.490	0.710953	26	0.703239
T	1100	9.133	60.91	0.09070	0.511959	8	1.7	1476	1593						
Bhejripadar															
BP1	1100	10.058	78.00	0.07801	0.511906	10	2.4	1398	1531						
Kodomali															
K4	480	8.525	73.88	0.06980	0.512343	10	2.0	857	1058						
K7	480	10.46	80.13	0.07894	0.512325	10	1.1	935	1134	80.67	1079	0.216	0.707866	20	0.706387
Majhgawan															
M	1100	26.73	230.8	0.07007	0.511742	10	0.4	1494	1703						
KM1	1100	26.97	226.3	0.07206	0.511753	7	0.3	1503	1709	128.4	1029	0.361	0.709534	21	0.703855
KM2	1100	32.52	294.3	0.06679	0.511715	6	0.3	1488	1709	105.4	1095	0.278	0.708326	20	0.703943
KM3	1100	24.22	184.1	0.07951	0.511808	6	0.3	1524	1707	77.35	1226	0.183	0.706772	18	0.703899

ϵ parameter was calculated in reference to CHUR values: $^{147}\text{Sm}/^{144}\text{Nd}=0.1967$, $^{143}\text{Nd}/^{144}\text{Nd}=0.512638$.

Model ages T(DM) and T(DM2) were calculated assuming the following DM parameters: $^{147}\text{Sm}/^{144}\text{Nd}=0.2136$, $^{143}\text{Nd}/^{144}\text{Nd}=0.513151$; continental crust: $^{147}\text{Sm}/^{144}\text{Nd}=0.12$.